High-Gain InAs Planar Avalanche Photodiodes

Benjamin S. White, Ian C. Sandall, Xinxin Zhou, Andrey Krysa, Kenneth McEwan,
John P. R. David, *Fellow, IEEE*, and Chee Hing Tan, *Member, IEEE*

***Abstract*—We report the fabrication of InAs planar avalanche photodiodes (APDs) using Be ion implantation. The planar APDs have a low background doping of $2 \times 10^{14}\,\mathrm{cm}^{-3}$ and large depletion widths approaching 8 μm. The thick depletion width enabled a gain of 330 to be achieved at -26 V at 200 K without inducing a significant tunneling current. No edge breakdown was observed within the APDs. The surface leakage current was found to be low with a gain normalized dark current density of 400 $\mu\mathrm{Acm}^{-2}$ at -20 V at 200 K.**

***Index Terms*—Avalanche photodiodes, infrared detectors, ion implantation.**

I. Introduction

AVALANCHE photodiodes (APDs) can improve receiver sensitivity by amplifying the photo-generated carriers through a cascade of impact ionisation events. APDs are frequently employed in photon starved applications across the infrared spectral region due to eye-safe consideration, the presence of atmospheric transmission windows, and the unique absorption signature of molecular bonds which can be used for remote chemical sensing. The performance of HgCdTe APDs exceeds all other commercial APDs for detecting few infrared photons, achieving high quantum efficiency across the entire short-wave infrared (SWIR) and mid-wave infrared (MWIR) spectral regions with high gain and near ideal excess noise characteristics [1]. However, to minimise crystal defects, HgCdTe APDs are grown on CdZeTe substrates which are costly and unavailable in large formats [2]. Furthermore, low device yields relative to mature III-V semiconductors and the requirement of cryogenic temperature operation culminate in exceptionally high costs for HgCdTe APDs [2]. Despite being limited by poor excess noise performance, InGaAs/InP APDs are thoroughly favoured over HgCdTe APDs for photon starved SWIR applications due the convenience of room temperature operation and low manufacturing costs. An affordable alternative to the MWIR HgCdTe APD is also highly desirable and in recent years InAs APDs have been developed with this intent. Recently InAs APDs have in-part boasted similar performance to HgCdTe APDs achieving high avalanche gain with an excess noise factor below 2 [3], a bandwidth of several GHz which is independent of APD gain [4] and high quantum efficiency over the spectral region of 1.55 to 3.5 μm [5]. However, the full potential of the InAs APD is realised when considering the low production costs, due to readily accessible III-V fabrication facilities and relatively cheap 3" native substrates, but also the potential for operating InAs APDs at temperatures of $\sim$200 K using Peltier cooling to drastically reduce system costs, complexity and size [6].

Historically the surface leakage of InAs has been difficult to control, and although wet chemical etching recipes have been developed to reduce the surface leakage [7], complete removal of surface leakage current in small area mesa APDs remains a challenge. The development of an InAs planar APD is desirable as the planar topology benefits from a simplified and economic fabrication process with high manufacturing yields, device uniformity and reliability, and excellent control over surface conditions; as evident from the maturing of Si, InGaAs/InP and HgCdTe APD technologies [8], [9]. Additionally, the wet chemical etching process used to fabricate mesa InAs APDs produces a bevel angle of approximately 45° [7]. The acute bevel angle complicates the fabrication of small area APDs with thick avalanche regions due to mask undercutting and limits the detector pitch and fill factor for array applications. Recently, InAs planar photodiodes fabricated using Be implantation have shown bulk dominated dark current characteristics and good electrical isolation [10] laying the pathway to large format array fabrication.

In this paper we report InAs planar APDs fabricated using Be ion implantation. The planar APDs showed low surface leakage and displayed a diffusion dominated dark current down to a temperature of 200 K achieving a dark current density of 400 $\mu\mathrm{Acm}^{-2}$ at 200 K. A low background doping of 2×10^{14} cm^{-3} and a depletion width of 8 μm were achieved in the planar APDs which were grown using metalorganic vapour phase epitaxy (MOVPE). The low background doping and wide depletion widths enabled a gain of 330 to be obtained at -26 V at 200 K without incurring a significant tunnelling current. The gain characteristics of the planar APD were found to be comparable to a HgCdTe APD with a similar cut-off wavelength operating at 200 K [11]. A graded p-type region successfully prevented edge breakdown within the APDs without the requirement of fabricating guard rings or isolation trenches.

II. Fabrication

InAs was grown using MOVPE with a susceptor temperature of 590 °C and consisted of a 10 μm thick undoped layer on a 500 nm thick N type layer doped to 5×10^{17} cm^{-3} with Si grown

Manuscript received December 15, 2015; revised January 28, 2016; accepted February 11, 2016. This work was supported in part by the European Space Agency under Grant 4000107110, in part by the Engineering and Physical Sciences Research Council under Grant EP/H031464/1, in part by a LAND CASE studentship, and in part by the Defence Science and Technology Laboratory under Grant DSTLX1000064084.

B. S. White, I. Sandall, X. Zhou, A. Krysa, J. P. R. David, and C. H. Tan are with the Department of Electronic and Electrical Engineering, University of Sheffield, Sheffield S1 3JD, U.K. (e-mail: ben.white@sheffield.ac.uk; i.sandall@sheffield.ac.uk; x.zhou@sheffield.ac.uk; a.krysa@sheffield.ac.uk; j.p.david@sheffield.ac.uk; c.h.tan@sheffield.ac.uk).

K. McEwan is with the Defence Science and Technology Laboratory, Salisbury SP4 0JQ, U.K. (e-mail: klmcewan@mail.dstl.gov.uk).

Color versions of one or more of the figures in this paper are available online at http://ieeexplore.ieee.org.

Digital Object Identifier 10.1109/JLT.2016.2531278

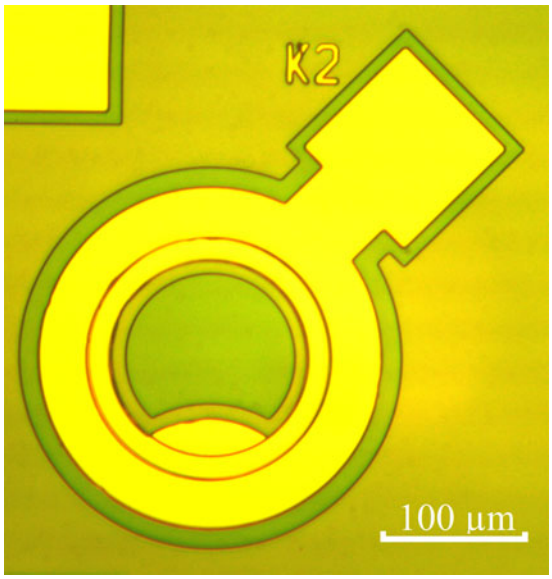

Fig. 1. A photograph of a fabricated InAs planar APD with a remote bondpad

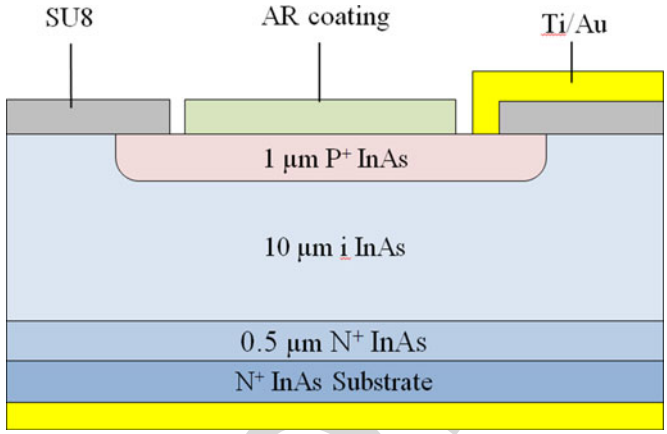

Fig. 2. A schematic diagram of an InAs planar APD.

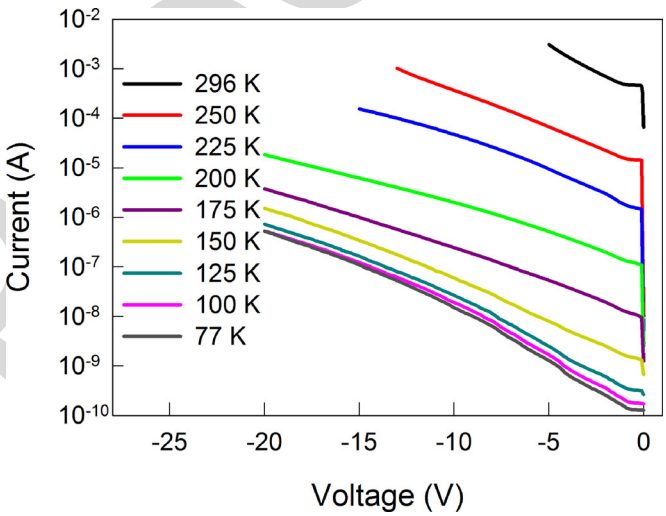

Fig. 3. The temperature dependence of current-voltage characteristics of a 200 μm diameter planar APD.

on a (100) N^+ InAs substrate. The growth rate was initially set at 3.8 $Å s^{-1}$ for 46 nm before being increased to 7.6 $Å s^{-1}$ for the remainder of the structure. A slow initial growth rate was employed to planarize the substrate and help reduce the defect nucleation rate which can be exacerbated by the roughness of the polished substrate. Compared to previous work in [10], a thick intrinsic region was employed to increase the depletion width and achieve high gain from the APD. A 35 nm layer of SiO_2 was deposited by plasma-enhanced chemical vapor deposition (PECVD) onto the surface of the wafer at 300 °C before the wafer was patterned with 4 μm of photoresist to expose circular regions with radii ranging from 7.5 to 200 μm. The wafer was implanted with Be at room temperature, 7° off axis using implant conditions of 1×10^{14} cm^{-2} at 200 keV and 3.8×10^{13} cm^{-2} at 70 keV to produce a 1 μm deep P^+ region. After implantation the photoresist was removed and the wafer was annealed at 550 °C for 30 s in a nitrogen rich atmosphere to recover the crystal [10]. The annealing caused significant Be diffusion away from the surface of the wafer and considerably increased the thickness of the P^+ region. Improvements to the device performance compared to [10] were achieved by removing the SiO_2 film before SiN bondpads and single layer anti-reflective (AR) coating optimised for absorption at 2 μm were deposited at 300 °C by PECVD. The remaining surface around the APD was passivated with 3.5 μm of SU-8. Ti/Au back and top contacts were deposited overlapping the SU8 passivation to ensure a pure injection of photon when performing gain measurements. A photograph and a schematic diagram of an InAs planar APD are shown in Fig. 1 and 2 respectively.

III. Results

The current-voltage (I-V) characteristics of a nominal 200 μm diameter planar APD are shown in Fig. 3 at temperature intervals from 296 to 77 K. The dark current density of the 200 μm diameter planar APD was found to be approximately 1.3 Acm^{-2} at room temperature and 400 μAcm^{-2} at 200 K which is similar to the value reported for planar InAs photodiodes [10]. APDs with nominal diameters ranging from 400 to 50 μm were also measured at each temperature interval and used to calculate the bulk and surface leakage current at -0.4 V using a technique described in [12]. An example of the fit used to calculate the bulk and surface leakage components of the dark current at 296 K is shown in Fig. 4. The dark current for each diode was taken at -0.4 V before avalanche gain became significant. A good fit of the room temperature dark current was achieved from a bulk current density of 1.3 Acm^{-2} and surface leakage (normalized to device perimeter) of 4×10^{-4} Acm^{-1}. Diodes with diameters of 15 and 20 μm were also measured at 296 K and are shown in Fig. 4 for comparison. A good fit could not be achieved when including diodes with diameters of 15 and 20 μm in the analysis. The active area of the planar APD was assumed to be the area implanted with Be, however, Be has been shown to diffuse

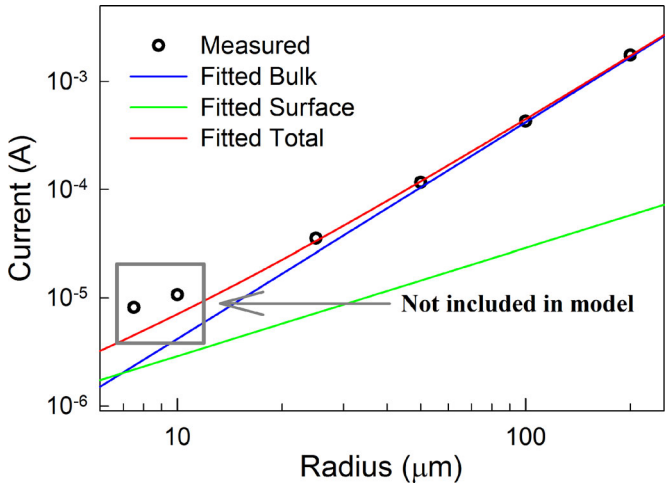

Fig. 4. The dark current of planar InAs APDs with various radii at −0.4 V at 296 K. Empirical fitting has been used to model the bulk and surface leakage components of the total dark current of diodes with radii greater than 10 μm. The dark current of diodes with radii of 7.5 and 10 μm are included to highlight the significance of lateral Be diffusion.

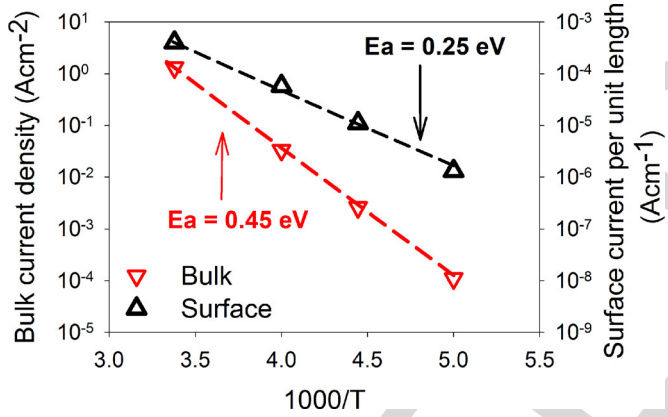

Fig. 5. An Arrhenius plot of the bulk and surface leakage currents of the APD at temperatures of 296, 250 225 and 200 K shown by the symbols. A linear fit of the bulk and surface leakage currents is shown by the dashed line used to calculate the activation energy.

during annealing in InAs, and could significantly increase the active area of the small APDs.

The bulk and surface leakage components of the dark current were calculated at 296, 250, 225 and 200 K at −0.4 V with the results plotted against the inverse of temperature as shown in Fig. 5. The activation energy, E_a, of the bulk and surface leakage current was calculated by fitting the respective current to Eq. (1),

$$I_d = T^2 \exp\left(-E_a/kT\right) \quad (1)$$

where T is the absolute temperature and k is the Boltzmann constant yielding values of 0.45 eV and 0.25 eV respectively. The 15 and 20 μm diodes were not included in the analysis. The activation energy of the bulk leakage mechanism is slightly larger than the low temperature bandgap of InAs and is therefore interpreted as a diffusion current. The discrepancy between

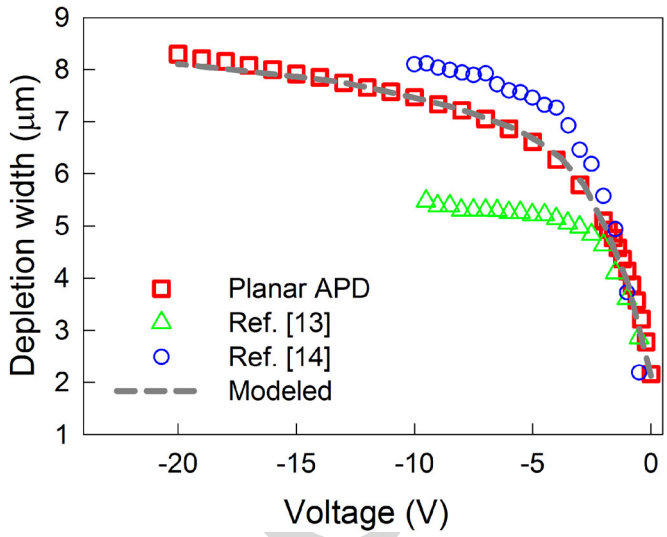

Fig. 6. The measured depletion width vs reverse bias voltage characteristics of planar InAs APDs as deduced from capacitance-voltage measurements taken at 77 K in comparison with data from [13] and [14]. The simulated depletion width vs reverse bias voltage characteristics of the APD structure are also shown.

the activation energy and the bandgap of InAs could be due to slight errors in determining the APD temperature or, the pre-exponential term of (1) having a larger temperature dependence than assumed. However, the bulk leakage activation energy measured here is similar to values reported for mesa InAs APDs [3], [12]. The surface leakage activation energy is closer to a value of half the bandgap indicating contribution from a generation-recombination process. At temperatures below 200 K the surface leakage became significant enough to cause large errors when determining the true value of the bulk leakage current and so the analysis was stopped. Additionally, the background induced photocurrent (300 K thermal radiation) became significant at 150 K further complicating the analysis at lower temperatures.

Thick avalanche regions with low background doping are required to achieve high gain in InAs APDs [6]. Typically the depletion width of InAs APDs has been limited to 6 um [13], however, recently a depletion width of 8 μm has been demonstrated [14]. Fig. 6 shows the depletion width versus reverse bias voltage characteristics of the planar APD as determined from Capacitance-Voltage (C-V) measurements at 77 K. The depletion width of the APD approached 8 μm at −20 V which is similar to the maximum depletion width reported for a mesa InAs APD [14]. To complement the C-V profiling analysis, Be and Si doping concentrations were measured using secondary ion mass spectrometry (SIMS) with the results shown in Fig. 7. Be was implanted to a depth of 1 μm, however, the 550 °C anneal has driven the Be deeper into the APD forming a graded p-type region extending to a depth of 2 μm until the noise floor of the SIMS measurement was reached. Although the Be diffusion narrows the intrinsic region of the device, the graded p-type doping is desirable as the peak electric field within the APD is reduced due the low doping density at the junction. The graded p-type doping also increasing the curvature of the spherical planar junction and alleviates the effects edge breakdown.

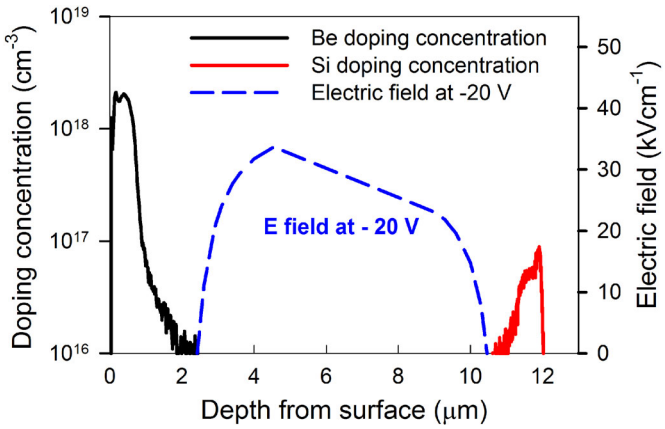

Fig. 7. SIMS measurements of the Be and Si doping concentrations as a function of distance from the wafer surface. The electric field developed across the avalanche region of the APD at −20 V is also shown.

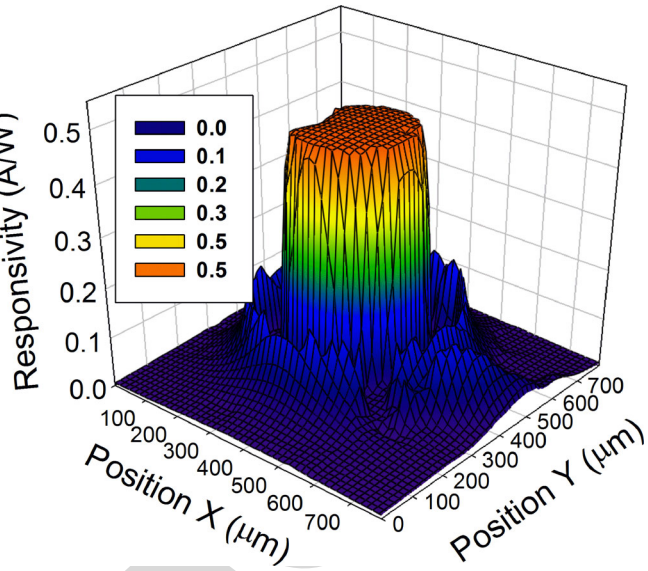

Fig. 8. The spatial responsivity of a 400 μm diameter planar APD at −0.3 V at 296 K in response to 1550 nm wavelength light.

Additionally, the thicker p-type region improves the excess noise performance of the APD by decreasing mixed injection. With the knowledge of the diffusion rate of Be in InAs, the p-type grading of an APD could easily be tailored for specific applications by selecting an adequate annealing time to control the Be diffusion depth addressing both high gain and narrow pitch applications. Si is known to be static in InAs during annealing [15], however, the Si dopants were traced into the intrinsic layer. As the Si tail only extends in the direction of epitaxial growth, parasitic incorporation of residual Si dopants from the reactor's chamber walls are suspected to cause the Si tail. Low background doping in the intrinsic region is required to maintain a uniform electric field across the avalanche region without inducing high tunnelling currents. As both the P and N type doping profiles have shallow gradients, the background doping of the wafer was found by modelling the C-V characteristics of the APD using a one–dimensional Poisson solver rather than calculating the background doping from the incremental depletion width and assuming a one sided abrupt junction. The Si and Be doping concentrations within the APD were extrapolated from the SIMS measurements following the roll off of the diffusion tail down to the background doping level which was assumed to be n-type. An excellent fit between the experimental data and the modelled C-V characteristics is obtained for an intrinsic region background doping of 2×10^{14} cm^{-3} as shown in Fig. 6. With knowledge of the doping profile, the electric field within the APD was generated at −20 V as shown in Fig. 7. The electric field is seen to be relatively flat across the device with the peak value reaching 33.5 kVcm^{-1} which is far below the value at which hole impact ionisation and tunnelling current can become significant in InAs APDs at 70 kVcm^{-1} [6]. Due to the p-type doping of the planar APD being added post growth, excellent control of the doping profile and lower levels of background doping have been achieved from the planar structure resulting in very low background doping sustained over a large width. Previous reports of low background doping in InAs (below 5×10^{14} cm^{-3}) have been achieved using Molecular Beam Epitaxy (MBE) which was preferred over MOVPE for reducing the incorporation of dicarbon deep-donors which are present in the MOVPE former [13]. However, the background doping level reported here is equal to lowest level reported using MBE growth [13]. The source of the background doping in the planar APDs was not determined. Since the growth of thick avalanche regions with low background doping are required for high gain InAs APDs [6], the development of planar APDs grown using MOVPE rather than relying on MBE techniques is a welcoming development for targeting the lower cost APD market rivalling HgCdTe.

Gain and responsivity measurements were performed using phase sensitive detection with a 1550 nm laser focused onto the p-type region of the APD. The responsivity was found to be 0.46 A/W at 296 K. Photocurrent shunting can cause non-uniform responsivity across large area InAs photodiodes [16]. The shunt resistance of a planar APD with a diameter of 400 μm was found to be 57 Ω when measured between 0 to −0.1 V and 1.37 kΩ between −0.2 to −0.3 V. The series resistance was measured to be less than 15 Ω. The spatial responsivity of a 400 μm diameter planar InAs APD was mapped at room temperature at −0.3 V and was found to have a uniform responsivity as shown in Fig. 8. The gain of a 200 μm diameter APD was measured to be 5 at −4.5 V at room temperature. The gain at 200 K is shown in Fig. 9 with a gain of 330 being achieved at −26 V. The gain from a mesa InAs APD and a $Hg_{0.62}Cd_{0.38}Te$ APD operating at 200 K with a corresponding cut off wavelength 3.21 μm are shown for comparison [17], [11]. Since the gain of an InAs APD is strongly dependant on the intrinsic region thickness, the gain of the planar APD reported here is the largest reported for an InAs planar APD. Furthermore, the gain is shown to be comparable with a state of the art $Hg_{0.62}Cd_{0.38}Te$ APD of similar cutoff wavelength. The graded p-type doping prevented edge breakdown by reducing the peak electric field as demonstrated in Fig. 7. Consequently no edge breakdown

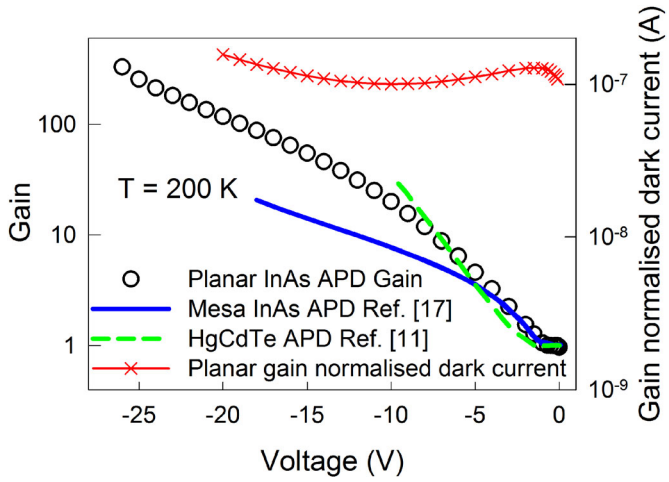

Fig. 9. The gain of a planar APD measured at 200 K using a 1550 nm laser in comparison to data from [11] and [17]. The gain normalised dark current of a 200 μm diameter planar APD is also shown at 200 K.

was observed from the any of the planar APDs when measuring the gain characteristics. Additionally, the low electric field maintained across the large depletion width supressed the generation of tunnelling current within the APD at high biases. The gain normalised dark current of a 200 μm diameter APD is shown in Fig. 9 at 200 K and was found to remain relatively flat through the voltage range measured indicating that the dark current is multiplied at the approximately the same rate as the gain. The dark current is therefore believed to be a diffusion current from the p-type region of the device. Additionally, due to the flatness of the gain normalised dark current, we can also conclude that the surface leakage of the APD is low at large bias voltages at 200 K.

IV. Discussion

We have established that the bulk leakage current in InAs planar APDs is generated by a diffusion process from the p-type region of the device within the temperature range of 296 to 200 K. The dark current of InAs mesa APDs is reported to behave in the same manner, however, the magnitude of the diffusion current from mesa APDs is generally lower than that of planar APDs reported here [12]. It has been argued that the diffusion current in mesa APDs is generated by thermionic emission of carriers from the p-type contact [7]. Recently a record low dark current from a mesa APD has been achieved by utilising a very highly doped p-type surface layer to reduce thermionic emission [13]. By comparison the surface layer of our planar APD is lowly doped, and therefore the thermionic emission would be very large. However, a more likely cause for the increased leakage current of the planar APD is due to the minority carrier diffusion length in the p-type material being low compared to epitaxially grown material. Defects caused by Be implantation could be causing this lower value. Optimisation of the implantation conditions to minimise implant damage, or the use of diffusion techniques may therefore significantly reduce the dark current of the planar APDs. A similar analysis holds for the responsivity of the planar APDs which is slightly lower than reports of mesa APDs at 1550 nm [5].

The planar fabrication process allowed good control of the surface conditions and consequently low surface leakage compared to other reports of mesa InAs APDs. However, surface leakage was still significant, particularly at low temperatures or in small devices. The surface leakage has been largely eliminated from planar InGaAs/InP and HgCdTe APDs by incorporating a wide bandgap lattice matched surface layer grown in-situ to achieve a high quality interface [18] [9]. Lattice matched wide bandgap alloys, such as AlAsSb and GaAsSb, are available to InAs which could potentially operate in a similar manner. Furthermore, by moving the p-region to a wide-bandgap material, the diffusion current would be significantly reduced which could result in planar InAs APDs operating with very low dark currents. However, it is noted that by utilising a wide bandgap p-type layer, the infrared wavelengths would be absorbed within the intrinsic region of the APD causing a slight increase in excess noise and decrease in the gain.

V. Conclusion

In this paper we report the fabrication of planar InAs APDs. The dominant leakage mechanism of the planar APDs was by a diffusion of carriers from the p-type region in the temperature range of 296 to 200 K. The surface leakage was low with the diffusion current dominating the dark current of a 200 μm diameter device at -20 V at 200 K. C-V characterisation of the planar APDs revealed a low background doping of 2×10^{14} cm^{-3} was achieved with depletion widths as large as $\sim$8 μm. Consequently the planar APDs displayed a very high gain of 330 at -26 V at 200 K. A graded p-type region was incorporated into the APD structure to prevent edge breakdown at high operating biases. The low background doping and low surface leakage was attributed to the benefits of the planar fabrication process.

References

[1] J. D. Beck, R. Scritchfield, P. Mitra, W. W. Sullivan, A. D. Gleckler, R. Strittmatter, and R. J. Martin, "Linear mode photon counting with the noiseless gain HgCdTe e-avalanche photodiode," *Opt. Eng.*, vol. 53, no. 8, p. 081905, 2014.

[2] F. Aqariden, J. Elsworth, J. Zhao, C. H. Grein, and S. Sivananthan, "MBE HgCdTe for HDVIP Devices: Horizontal Integration in the US HgCdTe FPA Industry," *J. Electron. Mater.*, vol. 41, no. 10, pp. 2700–2706, Aug. 2012.

[3] W. Sun, Z. Lu, X. Zheng, J. C. Campbell, S. J. Maddox, H. P. Nair, and S. R. Bank, "High-Gain InAs avalanche photodiodes," *IEEE J. Quantum Electron.*, vol. 49, no. 2, pp. 154–161, Dec. 2012.

[4] A. R. J. Marshall, P. J. Ker, A. Krysa, J. P. R. David, and C. H. Tan, "High speed InAs electron avalanche photodiodes overcome the conventional gain-bandwidth product limit.," *Opt. Exp.*, vol. 19, no. 23, pp. 23341–23349, Nov. 2011.

[5] X. Zhou, X. Meng, A. Krysa, J. Willmott, J. S. Ng, and C. H. Tan, "InAs photodiodes for 3.43 μm radiation thermometry," *IEEE Sens. J.*, vol. 15, no. 10, pp. 5555–5560, Jun. 2015.

[6] A. Marshall, P. Vines, P. J. Ker, J. P. R. David, and C. H. Tan, "Avalanche multiplication and excess noise in InAs electron avalanche photodiodes at 77 K," *IEEE J. Quantum Electron.*, vol. 47, no. 6, pp. 858–864, Jun. 2011.

[7] A. R. J. Marshall, C. H. Tan, J. P. R. David, J. S. Ng, and M. Hopkinson, "Fabrication of InAs photodiodes with reduced surface leakage current," *Proc. SPIE, Opt. Mater. Defence Syst. Technol. IV*, vol. 6740, p. 67400H, 2007.

[8] B. R. H. Saul, F. S. Chen, and P. W. Shumate, "Reliability of InGaAs photodiodes for SL applications," *AT&T Tech. J.*, vol. 64, no. 3, pp. 861–882, 1985.

[9] J. M. Arias, J. G. Pasko, M. Zandian, S. H. Shin, G. M. Williams, L. O. Bubulac, R. E. Dewames, and W. E. Tennant, "Planar p-on-n HgCdTe heterostructure photovoltaic detectors," *Appl. Phys. Lett.*, vol. 62, no. 9, pp. 976–978, 1993.

[10] B. S. White, I. C. Sandall, J. P. R. David, and C. H. Tan, "InAs diodes fabricated using be ion implantation," *IEEE Trans. Electron Devices*, vol. 62, no. 9, pp. 2928–2932, Aug. 2015.

[11] J. Rothman, L. Mollard, S. Bosson, G. Vojetta, K. Foubert, S. Gatti, G. Bonnouvrier, F. Salveti, A. Kerlain, and O. Pacaud, "Short-wave infrared HgCdTe avalanche photodiodes," *J. Electron. Mater.*, vol. 41, no. 10, pp. 2928–2936, 2012.

[12] P. J. Ker, A. R. J. Marshall, A. B. Krysa, J. P. R. David, and C. H. Tan, "Temperature dependence of leakage current in InAs avalanche photodiodes," *J. Quantum Electron.*, vol. 47, no. 8, pp. 1123–1128, 2011.

[13] S. J. Maddox, W. Sun, Z. Lu, H. P. Nair, J. C. Campbell, and S. R. Bank, "Enhanced low-noise gain from InAs avalanche photodiodes with reduced dark current and background doping," *Appl. Phys. Lett.*, vol. 101, no. 15, p. 151124, 2012.

[14] W. Sun, S. J. Maddox, S. R. Bank, and J. C. Campbell, "Record high gain from InAs avalanche photodiodes at room temperature," in *Proc. 72nd Annu. Device Res. Conf.*, Santa Barbara, CA, USA, 2014, pp. 47–48.

[15] S. J. Pearton, A. R. Von Neida, J. M. Brown, K. T. Short, and L. J. Oster, "Ion implantation damage and annealing in InAs, GaSb, and GaP," *J. Appl. Phys.*, vol. 64, no. 2, pp. 629–636, 1988.

[16] (Mar. 2003). *J12 Indium Arsenide Detectors*, Teledyne Judson Technologies LLC, Montgomeryville, PA, USA. [Online]. Available: http://www.judsontechnologies.com/files/pdf/InAs_shortform_Mar2003.pdf

[17] P. J. Ker, J. P. R. David, and C. H. Tan, "Temperature dependence of gain and excess noise in InAs electron avalanche photodiodes," *Opt. Exp.*, vol. 20, no. 28, pp. 1123–1128, Dec. 2012.

[18] B. Dutt, R. McCoy, and J. Zuber, "A low dark-current, planar InGaAs p-i-n photodiode with a quaternary InGaAsP cap layer," *IEEE J. Quantum Electron.*, vol. QE-21, no. 2, pp. 138–143, Feb. 1985.

Authors' biographies not available at the time of publication.

High-Gain InAs Planar Avalanche Photodiodes

Benjamin S. White, Ian C. Sandall, Xinxin Zhou, Andrey Krysa, Kenneth McEwan,
John P. R. David, *Fellow, IEEE*, and Chee Hing Tan, *Member, IEEE*

***Abstract*—We report the fabrication of InAs planar avalanche photodiodes (APDs) using Be ion implantation. The planar APDs have a low background doping of $2 \times 10^{14}\,\mathrm{cm}^{-3}$ and large depletion widths approaching 8 μm. The thick depletion width enabled a gain of 330 to be achieved at -26 V at 200 K without inducing a significant tunneling current. No edge breakdown was observed within the APDs. The surface leakage current was found to be low with a gain normalized dark current density of 400 $\mu\mathrm{Acm}^{-2}$ at -20 V at 200 K.**

***Index Terms*—Avalanche photodiodes, infrared detectors, ion implantation.**

I. Introduction

AVALANCHE photodiodes (APDs) can improve receiver sensitivity by amplifying the photo-generated carriers through a cascade of impact ionisation events. APDs are frequently employed in photon starved applications across the infrared spectral region due to eye-safe consideration, the presence of atmospheric transmission windows, and the unique absorption signature of molecular bonds which can be used for remote chemical sensing. The performance of HgCdTe APDs exceeds all other commercial APDs for detecting few infrared photons, achieving high quantum efficiency across the entire short-wave infrared (SWIR) and mid-wave infrared (MWIR) spectral regions with high gain and near ideal excess noise characteristics [1]. However, to minimise crystal defects, HgCdTe APDs are grown on CdZeTe substrates which are costly and unavailable in large formats [2]. Furthermore, low device yields relative to mature III-V semiconductors and the requirement of cryogenic temperature operation culminate in exceptionally high costs for HgCdTe APDs [2]. Despite being limited by poor excess noise performance, InGaAs/InP APDs are thoroughly favoured over HgCdTe APDs for photon starved SWIR applications due the convenience of room temperature operation and low manufacturing costs. An affordable alternative to the MWIR HgCdTe APD is also highly desirable and in recent years InAs APDs have been developed with this intent. Recently InAs APDs have in-part boasted similar performance to HgCdTe APDs achieving high avalanche gain with an excess noise factor below 2 [3], a bandwidth of several GHz which is independent of APD gain [4] and high quantum efficiency over the spectral region of 1.55 to 3.5 μm [5]. However, the full potential of the InAs APD is realised when considering the low production costs, due to readily accessible III-V fabrication facilities and relatively cheap 3" native substrates, but also the potential for operating InAs APDs at temperatures of $\sim$200 K using Peltier cooling to drastically reduce system costs, complexity and size [6].

Historically the surface leakage of InAs has been difficult to control, and although wet chemical etching recipes have been developed to reduce the surface leakage [7], complete removal of surface leakage current in small area mesa APDs remains a challenge. The development of an InAs planar APD is desirable as the planar topology benefits from a simplified and economic fabrication process with high manufacturing yields, device uniformity and reliability, and excellent control over surface conditions; as evident from the maturing of Si, InGaAs/InP and HgCdTe APD technologies [8], [9]. Additionally, the wet chemical etching process used to fabricate mesa InAs APDs produces a bevel angle of approximately 45° [7]. The acute bevel angle complicates the fabrication of small area APDs with thick avalanche regions due to mask undercutting and limits the detector pitch and fill factor for array applications. Recently, InAs planar photodiodes fabricated using Be implantation have shown bulk dominated dark current characteristics and good electrical isolation [10] laying the pathway to large format array fabrication.

In this paper we report InAs planar APDs fabricated using Be ion implantation. The planar APDs showed low surface leakage and displayed a diffusion dominated dark current down to a temperature of 200 K achieving a dark current density of 400 $\mu\mathrm{Acm}^{-2}$ at 200 K. A low background doping of 2×10^{14} cm^{-3} and a depletion width of 8 μm were achieved in the planar APDs which were grown using metalorganic vapour phase epitaxy (MOVPE). The low background doping and wide depletion widths enabled a gain of 330 to be obtained at -26 V at 200 K without incurring a significant tunnelling current. The gain characteristics of the planar APD were found to be comparable to a HgCdTe APD with a similar cut-off wavelength operating at 200 K [11]. A graded p-type region successfully prevented edge breakdown within the APDs without the requirement of fabricating guard rings or isolation trenches.

II. Fabrication

InAs was grown using MOVPE with a susceptor temperature of 590 °C and consisted of a 10 μm thick undoped layer on a 500 nm thick N type layer doped to 5×10^{17} cm^{-3} with Si grown

Manuscript received December 15, 2015; revised January 28, 2016; accepted February 11, 2016. This work was supported in part by the European Space Agency under Grant 4000107110, in part by the Engineering and Physical Sciences Research Council under Grant EP/H031464/1, in part by a LAND CASE studentship, and in part by the Defence Science and Technology Laboratory under Grant DSTLX1000064084.

B. S. White, I. Sandall, X. Zhou, A. Krysa, J. P. R. David, and C. H. Tan are with the Department of Electronic and Electrical Engineering, University of Sheffield, Sheffield S1 3JD, U.K. (e-mail: ben.white@sheffield.ac.uk; i.sandall@sheffield.ac.uk; x.zhou@sheffield.ac.uk; a.krysa@sheffield.ac.uk; j.p.david@sheffield.ac.uk; c.h.tan@sheffield.ac.uk).

K. McEwan is with the Defence Science and Technology Laboratory, Salisbury SP4 0JQ, U.K. (e-mail: klmcewan@mail.dstl.gov.uk).

Color versions of one or more of the figures in this paper are available online at http://ieeexplore.ieee.org.

Digital Object Identifier 10.1109/JLT.2016.2531278

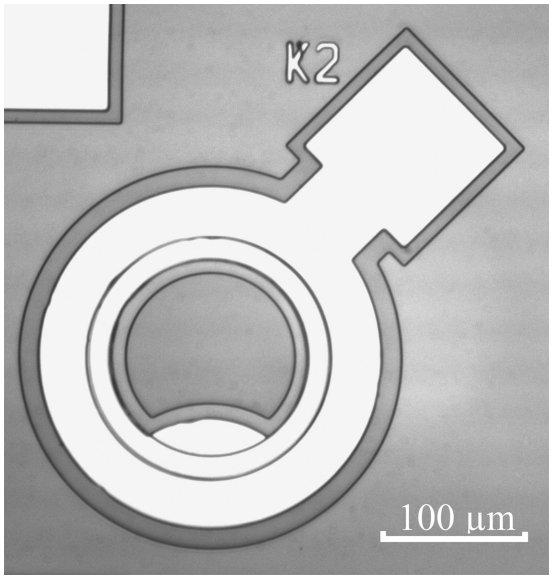

Fig. 1. A photograph of a fabricated InAs planar APD with a remote bondpad

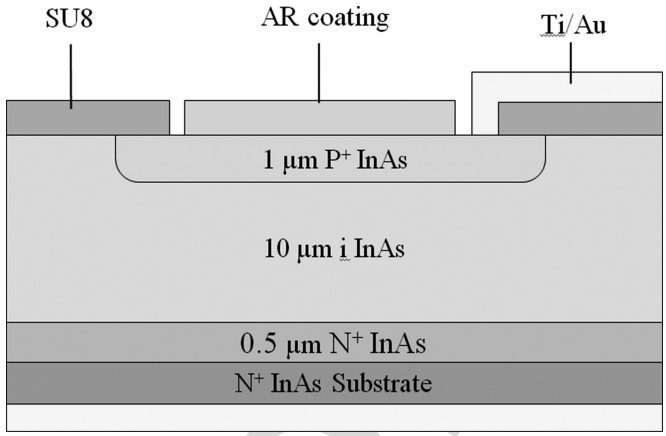

Fig. 2. A schematic diagram of an InAs planar APD.

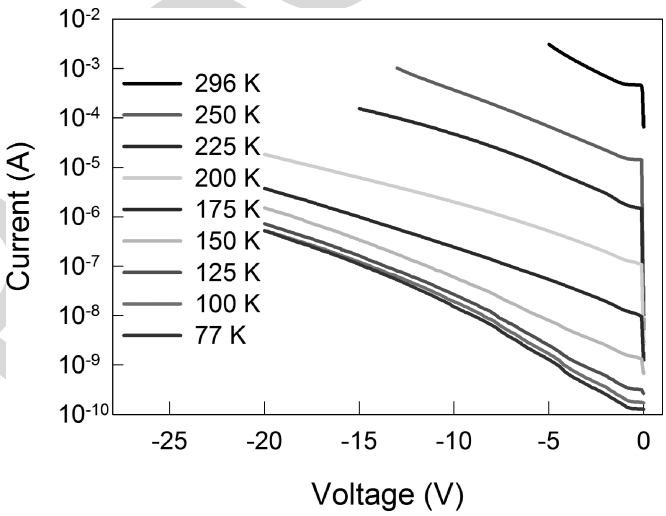

Fig. 3. The temperature dependence of current-voltage characteristics of a 200 μm diameter planar APD.

on a (100) N^+ InAs substrate. The growth rate was initially set at 3.8 $Å s^{-1}$ for 46 nm before being increased to 7.6 $Å s^{-1}$ for the remainder of the structure. A slow initial growth rate was employed to planarize the substrate and help reduce the defect nucleation rate which can be exacerbated by the roughness of the polished substrate. Compared to previous work in [10], a thick intrinsic region was employed to increase the depletion width and achieve high gain from the APD. A 35 nm layer of SiO_2 was deposited by plasma-enhanced chemical vapor deposition (PECVD) onto the surface of the wafer at 300 °C before the wafer was patterned with 4 μm of photoresist to expose circular regions with radii ranging from 7.5 to 200 μm. The wafer was implanted with Be at room temperature, 7° off axis using implant conditions of 1×10^{14} cm^{-2} at 200 keV and 3.8×10^{13} cm^{-2} at 70 keV to produce a 1 μm deep P^+ region. After implantation the photoresist was removed and the wafer was annealed at 550 °C for 30 s in a nitrogen rich atmosphere to recover the crystal [10]. The annealing caused significant Be diffusion away from the surface of the wafer and considerably increased the thickness of the P^+ region. Improvements to the device performance compared to [10] were achieved by removing the SiO_2 film before SiN bondpads and single layer anti-reflective (AR) coating optimised for absorption at 2 μm were deposited at 300 °C by PECVD. The remaining surface around the APD was passivated with 3.5 μm of SU-8. Ti/Au back and top contacts were deposited overlapping the SU8 passivation to ensure a pure injection of photon when performing gain measurements. A photograph and a schematic diagram of an InAs planar APD are shown in Fig. 1 and 2 respectively.

III. Results

The current-voltage (I-V) characteristics of a nominal 200 μm diameter planar APD are shown in Fig. 3 at temperature intervals from 296 to 77 K. The dark current density of the 200 μm diameter planar APD was found to be approximately 1.3 Acm^{-2} at room temperature and 400 μAcm^{-2} at 200 K which is similar to the value reported for planar InAs photodiodes [10]. APDs with nominal diameters ranging from 400 to 50 μm were also measured at each temperature interval and used to calculate the bulk and surface leakage current at -0.4 V using a technique described in [12]. An example of the fit used to calculate the bulk and surface leakage components of the dark current at 296 K is shown in Fig. 4. The dark current for each diode was taken at -0.4 V before avalanche gain became significant. A good fit of the room temperature dark current was achieved from a bulk current density of 1.3 Acm^{-2} and surface leakage (normalized to device perimeter) of 4×10^{-4} Acm^{-1}. Diodes with diameters of 15 and 20 μm were also measured at 296 K and are shown in Fig. 4 for comparison. A good fit could not be achieved when including diodes with diameters of 15 and 20 μm in the analysis. The active area of the planar APD was assumed to be the area implanted with Be, however, Be has been shown to diffuse

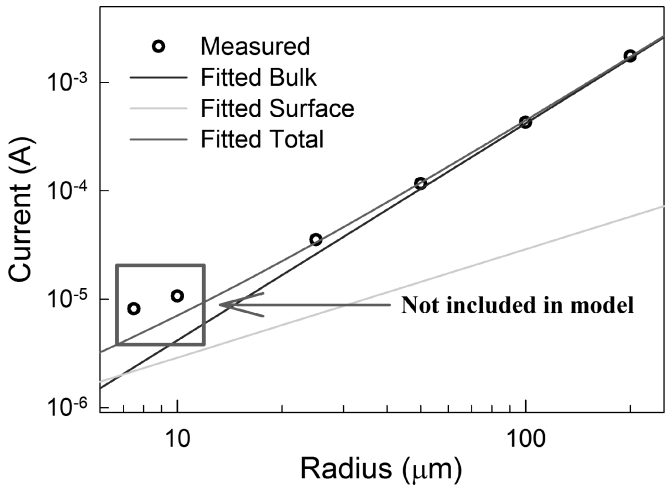

Fig. 4. The dark current of planar InAs APDs with various radii at −0.4 V at 296 K. Empirical fitting has been used to model the bulk and surface leakage components of the total dark current of diodes with radii greater than 10 μm. The dark current of diodes with radii of 7.5 and 10 μm are included to highlight the significance of lateral Be diffusion.

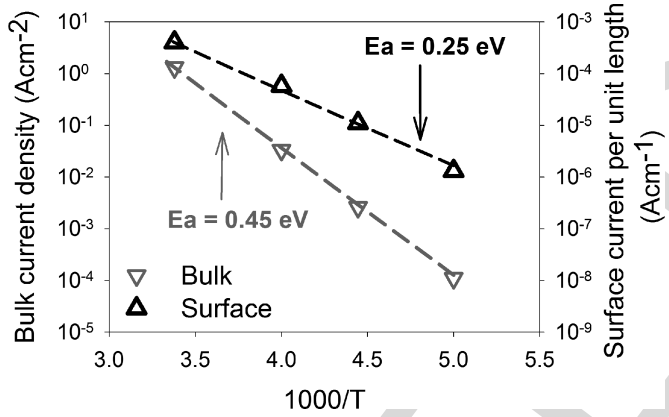

Fig. 5. An Arrhenius plot of the bulk and surface leakage currents of the APD at temperatures of 296, 250 225 and 200 K shown by the symbols. A linear fit of the bulk and surface leakage currents is shown by the dashed line used to calculate the activation energy.

during annealing in InAs, and could significantly increase the active area of the small APDs.

The bulk and surface leakage components of the dark current were calculated at 296, 250, 225 and 200 K at −0.4 V with the results plotted against the inverse of temperature as shown in Fig. 5. The activation energy, E_a, of the bulk and surface leakage current was calculated by fitting the respective current to Eq. (1),

$$I_d = T^2 \exp\left(-E_a/kT\right) \tag{1}$$

where T is the absolute temperature and k is the Boltzmann constant yielding values of 0.45 eV and 0.25 eV respectively. The 15 and 20 μm diodes were not included in the analysis. The activation energy of the bulk leakage mechanism is slightly larger than the low temperature bandgap of InAs and is therefore interpreted as a diffusion current. The discrepancy between

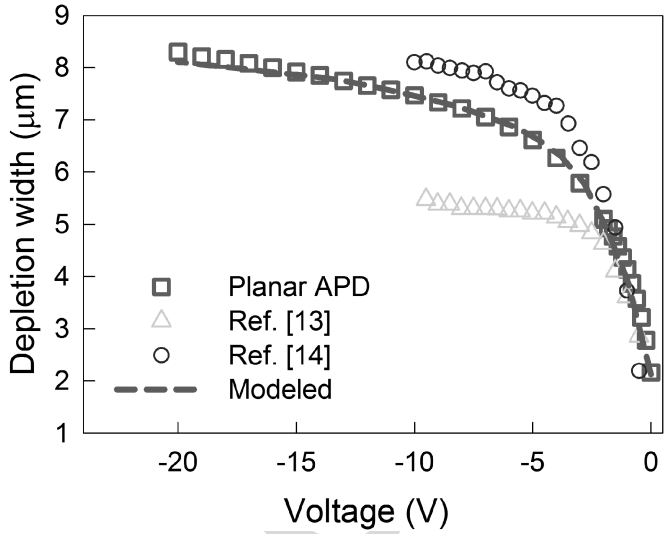

Fig. 6. The measured depletion width vs reverse bias voltage characteristics of planar InAs APDs as deduced from capacitance-voltage measurements taken at 77 K in comparison with data from [13] and [14]. The simulated depletion width vs reverse bias voltage characteristics of the APD structure are also shown.

the activation energy and the bandgap of InAs could be due to slight errors in determining the APD temperature or, the pre-exponential term of (1) having a larger temperature dependence than assumed. However, the bulk leakage activation energy measured here is similar to values reported for mesa InAs APDs [3], [12]. The surface leakage activation energy is closer to a value of half the bandgap indicating contribution from a generation-recombination process. At temperatures below 200 K the surface leakage became significant enough to cause large errors when determining the true value of the bulk leakage current and so the analysis was stopped. Additionally, the background induced photocurrent (300 K thermal radiation) became significant at 150 K further complicating the analysis at lower temperatures.

Thick avalanche regions with low background doping are required to achieve high gain in InAs APDs [6]. Typically the depletion width of InAs APDs has been limited to 6 um [13], however, recently a depletion width of 8 μm has been demonstrated [14]. Fig. 6 shows the depletion width versus reverse bias voltage characteristics of the planar APD as determined from Capacitance-Voltage (C-V) measurements at 77 K. The depletion width of the APD approached 8 μm at −20 V which is similar to the maximum depletion width reported for a mesa InAs APD [14]. To complement the C-V profiling analysis, Be and Si doping concentrations were measured using secondary ion mass spectrometry (SIMS) with the results shown in Fig. 7. Be was implanted to a depth of 1 μm, however, the 550 °C anneal has driven the Be deeper into the APD forming a graded p-type region extending to a depth of 2 μm until the noise floor of the SIMS measurement was reached. Although the Be diffusion narrows the intrinsic region of the device, the graded p-type doping is desirable as the peak electric field within the APD is reduced due the low doping density at the junction. The graded p-type doping also increasing the curvature of the spherical planar junction and alleviates the effects edge breakdown.

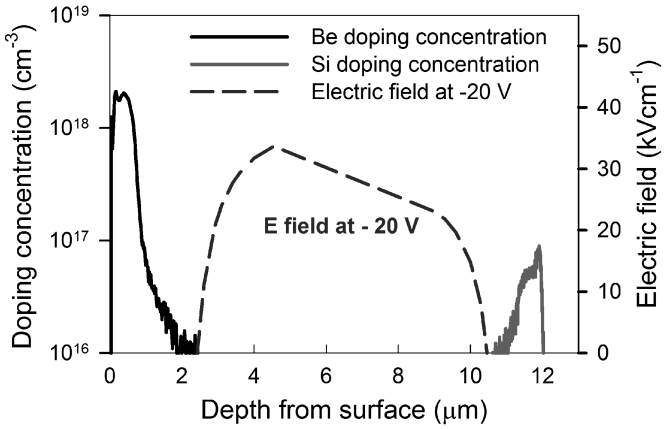

Fig. 7. SIMS measurements of the Be and Si doping concentrations as a function of distance from the wafer surface. The electric field developed across the avalanche region of the APD at −20 V is also shown.

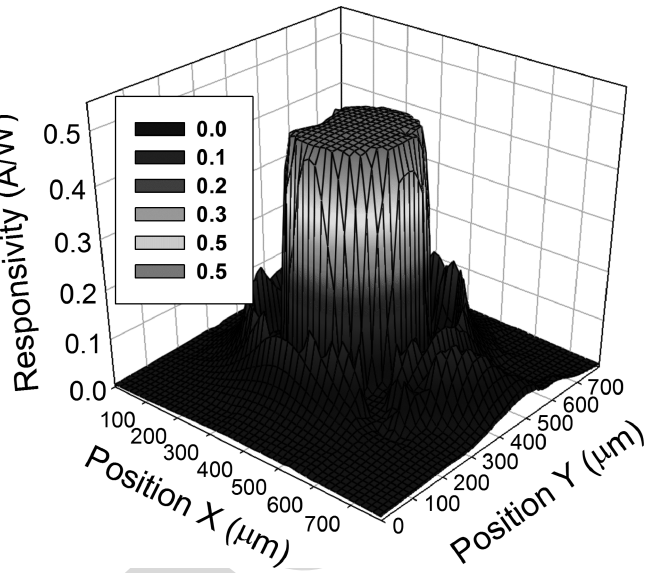

Fig. 8. The spatial responsivity of a 400 μm diameter planar APD at −0.3 V at 296 K in response to 1550 nm wavelength light.

Additionally, the thicker p-type region improves the excess noise performance of the APD by decreasing mixed injection. With the knowledge of the diffusion rate of Be in InAs, the p-type grading of an APD could easily be tailored for specific applications by selecting an adequate annealing time to control the Be diffusion depth addressing both high gain and narrow pitch applications. Si is known to be static in InAs during annealing [15], however, the Si dopants were traced into the intrinsic layer. As the Si tail only extends in the direction of epitaxial growth, parasitic incorporation of residual Si dopants from the reactor's chamber walls are suspected to cause the Si tail. Low background doping in the intrinsic region is required to maintain a uniform electric field across the avalanche region without inducing high tunnelling currents. As both the P and N type doping profiles have shallow gradients, the background doping of the wafer was found by modelling the C-V characteristics of the APD using a one–dimensional Poisson solver rather than calculating the background doping from the incremental depletion width and assuming a one sided abrupt junction. The Si and Be doping concentrations within the APD were extrapolated from the SIMS measurements following the roll off of the diffusion tail down to the background doping level which was assumed to be n-type. An excellent fit between the experimental data and the modelled C-V characteristics is obtained for an intrinsic region background doping of 2×10^{14} cm^{-3} as shown in Fig. 6. With knowledge of the doping profile, the electric field within the APD was generated at −20 V as shown in Fig. 7. The electric field is seen to be relatively flat across the device with the peak value reaching 33.5 kVcm^{-1} which is far below the value at which hole impact ionisation and tunnelling current can become significant in InAs APDs at 70 kVcm^{-1} [6]. Due to the p-type doping of the planar APD being added post growth, excellent control of the doping profile and lower levels of background doping have been achieved from the planar structure resulting in very low background doping sustained over a large width. Previous reports of low background doping in InAs (below 5×10^{14} cm^{-3}) have been achieved using Molecular Beam Epitaxy (MBE) which was preferred over MOVPE for reducing the incorporation of dicarbon deep-donors which are present in the MOVPE former [13]. However, the background doping level reported here is equal to lowest level reported using MBE growth [13]. The source of the background doping in the planar APDs was not determined. Since the growth of thick avalanche regions with low background doping are required for high gain InAs APDs [6], the development of planar APDs grown using MOVPE rather than relying on MBE techniques is a welcoming development for targeting the lower cost APD market rivalling HgCdTe.

Gain and responsivity measurements were performed using phase sensitive detection with a 1550 nm laser focused onto the p-type region of the APD. The responsivity was found to be 0.46 A/W at 296 K. Photocurrent shunting can cause non-uniform responsivity across large area InAs photodiodes [16]. The shunt resistance of a planar APD with a diameter of 400 μm was found to be 57 Ω when measured between 0 to −0.1 V and 1.37 kΩ between −0.2 to −0.3 V. The series resistance was measured to be less than 15 Ω. The spatial responsivity of a 400 μm diameter planar InAs APD was mapped at room temperature at −0.3 V and was found to have a uniform responsivity as shown in Fig. 8. The gain of a 200 μm diameter APD was measured to be 5 at −4.5 V at room temperature. The gain at 200 K is shown in Fig. 9 with a gain of 330 being achieved at −26 V. The gain from a mesa InAs APD and a $Hg_{0.62}Cd_{0.38}Te$ APD operating at 200 K with a corresponding cut off wavelength 3.21 μm are shown for comparison [17], [11]. Since the gain of an InAs APD is strongly dependant on the intrinsic region thickness, the gain of the planar APD reported here is the largest reported for an InAs planar APD. Furthermore, the gain is shown to be comparable with a state of the art $Hg_{0.62}Cd_{0.38}Te$ APD of similar cutoff wavelength. The graded p-type doping prevented edge breakdown by reducing the peak electric field as demonstrated in Fig. 7. Consequently no edge breakdown

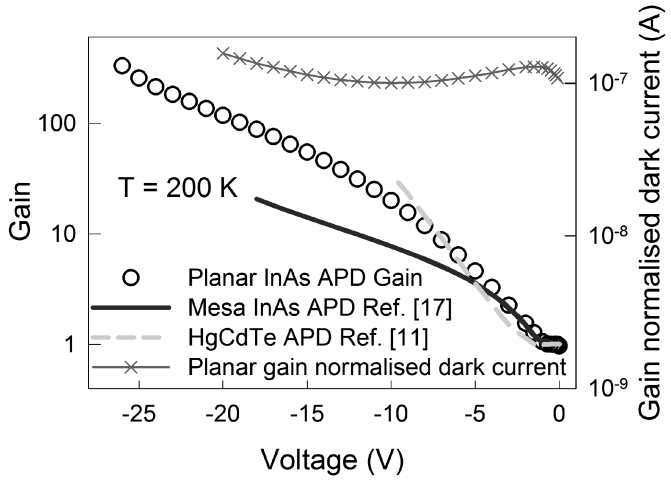

Fig. 9. The gain of a planar APD measured at 200 K using a 1550 nm laser in comparison to data from [11] and [17]. The gain normalised dark current of a 200 μm diameter planar APD is also shown at 200 K.

was observed from the any of the planar APDs when measuring the gain characteristics. Additionally, the low electric field maintained across the large depletion width supressed the generation of tunnelling current within the APD at high biases. The gain normalised dark current of a 200 μm diameter APD is shown in Fig. 9 at 200 K and was found to remain relatively flat through the voltage range measured indicating that the dark current is multiplied at the approximately the same rate as the gain. The dark current is therefore believed to be a diffusion current from the p-type region of the device. Additionally, due to the flatness of the gain normalised dark current, we can also conclude that the surface leakage of the APD is low at large bias voltages at 200 K.

IV. Discussion

We have established that the bulk leakage current in InAs planar APDs is generated by a diffusion process from the p-type region of the device within the temperature range of 296 to 200 K. The dark current of InAs mesa APDs is reported to behave in the same manner, however, the magnitude of the diffusion current from mesa APDs is generally lower than that of planar APDs reported here [12]. It has been argued that the diffusion current in mesa APDs is generated by thermionic emission of carriers from the p-type contact [7]. Recently a record low dark current from a mesa APD has been achieved by utilising a very highly doped p-type surface layer to reduce thermionic emission [13]. By comparison the surface layer of our planar APD is lowly doped, and therefore the thermionic emission would be very large. However, a more likely cause for the increased leakage current of the planar APD is due to the minority carrier diffusion length in the p-type material being low compared to epitaxially grown material. Defects caused by Be implantation could be causing this lower value. Optimisation of the implantation conditions to minimise implant damage, or the use of diffusion techniques may therefore significantly reduce the dark current of the planar APDs. A similar analysis holds for the responsivity of the planar APDs which is slightly lower than reports of mesa APDs at 1550 nm [5].

The planar fabrication process allowed good control of the surface conditions and consequently low surface leakage compared to other reports of mesa InAs APDs. However, surface leakage was still significant, particularly at low temperatures or in small devices. The surface leakage has been largely eliminated from planar InGaAs/InP and HgCdTe APDs by incorporating a wide bandgap lattice matched surface layer grown in-situ to achieve a high quality interface [18] [9]. Lattice matched wide bandgap alloys, such as AlAsSb and GaAsSb, are available to InAs which could potentially operate in a similar manner. Furthermore, by moving the p-region to a wide-bandgap material, the diffusion current would be significantly reduced which could result in planar InAs APDs operating with very low dark currents. However, it is noted that by utilising a wide bandgap p-type layer, the infrared wavelengths would be absorbed within the intrinsic region of the APD causing a slight increase in excess noise and decrease in the gain.

V. Conclusion

In this paper we report the fabrication of planar InAs APDs. The dominant leakage mechanism of the planar APDs was by a diffusion of carriers from the p-type region in the temperature range of 296 to 200 K. The surface leakage was low with the diffusion current dominating the dark current of a 200 μm diameter device at -20 V at 200 K. C-V characterisation of the planar APDs revealed a low background doping of 2×10^{14} cm^{-3} was achieved with depletion widths as large as $\sim$8 μm. Consequently the planar APDs displayed a very high gain of 330 at -26 V at 200 K. A graded p-type region was incorporated into the APD structure to prevent edge breakdown at high operating biases. The low background doping and low surface leakage was attributed to the benefits of the planar fabrication process.

References

[1] J. D. Beck, R. Scritchfield, P. Mitra, W. W. Sullivan, A. D. Gleckler, R. Strittmatter, and R. J. Martin, "Linear mode photon counting with the noiseless gain HgCdTe e-avalanche photodiode," *Opt. Eng.*, vol. 53, no. 8, p. 081905, 2014.

[2] F. Aqariden, J. Elsworth, J. Zhao, C. H. Grein, and S. Sivananthan, "MBE HgCdTe for HDVIP Devices: Horizontal Integration in the US HgCdTe FPA Industry," *J. Electron. Mater.*, vol. 41, no. 10, pp. 2700–2706, Aug. 2012.

[3] W. Sun, Z. Lu, X. Zheng, J. C. Campbell, S. J. Maddox, H. P. Nair, and S. R. Bank, "High-Gain InAs avalanche photodiodes," *IEEE J. Quantum Electron.*, vol. 49, no. 2, pp. 154–161, Dec. 2012.

[4] A. R. J. Marshall, P. J. Ker, A. Krysa, J. P. R. David, and C. H. Tan, "High speed InAs electron avalanche photodiodes overcome the conventional gain-bandwidth product limit.," *Opt. Exp.*, vol. 19, no. 23, pp. 23341–23349, Nov. 2011.

[5] X. Zhou, X. Meng, A. Krysa, J. Willmott, J. S. Ng, and C. H. Tan, "InAs photodiodes for 3.43 μm radiation thermometry," *IEEE Sens. J.*, vol. 15, no. 10, pp. 5555–5560, Jun. 2015.

[6] A. Marshall, P. Vines, P. J. Ker, J. P. R. David, and C. H. Tan, "Avalanche multiplication and excess noise in InAs electron avalanche photodiodes at 77 K," *IEEE J. Quantum Electron.*, vol. 47, no. 6, pp. 858–864, Jun. 2011.

[7] A. R. J. Marshall, C. H. Tan, J. P. R. David, J. S. Ng, and M. Hopkinson, "Fabrication of InAs photodiodes with reduced surface leakage current," *Proc. SPIE, Opt. Mater. Defence Syst. Technol. IV*, vol. 6740, p. 67400H, 2007.

[8] B. R. H. Saul, F. S. Chen, and P. W. Shumate, "Reliability of InGaAs photodiodes for SL applications," *AT&T Tech. J.*, vol. 64, no. 3, pp. 861–882, 1985.
[9] J. M. Arias, J. G. Pasko, M. Zandian, S. H. Shin, G. M. Williams, L. O. Bubulac, R. E. Dewames, and W. E. Tennant, "Planar p-on-n HgCdTe heterostructure photovoltaic detectors," *Appl. Phys. Lett.*, vol. 62, no. 9, pp. 976–978, 1993.
[10] B. S. White, I. C. Sandall, J. P. R. David, and C. H. Tan, "InAs diodes fabricated using be ion implantation," *IEEE Trans. Electron Devices*, vol. 62, no. 9, pp. 2928–2932, Aug. 2015.
[11] J. Rothman, L. Mollard, S. Bosson, G. Vojetta, K. Foubert, S. Gatti, G. Bonnouvrier, F. Salveti, A. Kerlain, and O. Pacaud, "Short-wave infrared HgCdTe avalanche photodiodes," *J. Electron. Mater.*, vol. 41, no. 10, pp. 2928–2936, 2012.
[12] P. J. Ker, A. R. J. Marshall, A. B. Krysa, J. P. R. David, and C. H. Tan, "Temperature dependence of leakage current in InAs avalanche photodiodes," *J. Quantum Electron.*, vol. 47, no. 8, pp. 1123–1128, 2011.
[13] S. J. Maddox, W. Sun, Z. Lu, H. P. Nair, J. C. Campbell, and S. R. Bank, "Enhanced low-noise gain from InAs avalanche photodiodes with reduced dark current and background doping," *Appl. Phys. Lett.*, vol. 101, no. 15, p. 151124, 2012.
[14] W. Sun, S. J. Maddox, S. R. Bank, and J. C. Campbell, "Record high gain from InAs avalanche photodiodes at room temperature," in *Proc. 72nd Annu. Device Res. Conf.*, Santa Barbara, CA, USA, 2014, pp. 47–48.
[15] S. J. Pearton, A. R. Von Neida, J. M. Brown, K. T. Short, and L. J. Oster, "Ion implantation damage and annealing in InAs, GaSb, and GaP," *J. Appl. Phys.*, vol. 64, no. 2, pp. 629–636, 1988.
[16] (Mar. 2003). *J12 Indium Arsenide Detectors*, Teledyne Judson Technologies LLC, Montgomeryville, PA, USA. [Online]. Available: http://www.judsontechnologies.com/files/pdf/InAs_shortform_Mar2003.pdf
[17] P. J. Ker, J. P. R. David, and C. H. Tan, "Temperature dependence of gain and excess noise in InAs electron avalanche photodiodes," *Opt. Exp.*, vol. 20, no. 28, pp. 1123–1128, Dec. 2012.
[18] B. Dutt, R. McCoy, and J. Zuber, "A low dark-current, planar InGaAs p-i-n photodiode with a quaternary InGaAsP cap layer," *IEEE J. Quantum Electron.*, vol. QE-21, no. 2, pp. 138–143, Feb. 1985.

Authors' biographies not available at the time of publication.